



Contents lists available at ScienceDirect

Journal of Non-Crystalline Solids

journal homepage: www.elsevier.com/locate/jnoncrystal

Co-based magnetic microwire and field-tunable multifunctional macro-composites

H.X. Peng^{a,*}, F.X. Qin^a, M.H. Phan^b, Jie Tang^c, L.V. Panina^d, M. Ipatov^e, V. Zhukova^e, A. Zhukov^e, J. Gonzalez^e^aAdvanced Composite Center for Innovation and Science, Department of Aerospace Engineering, University of Bristol, University Walk, Bristol BS8 1TR, UK^bPHY 221, Department of Physics, University of South Florida, 4202 E. Fowler Ave., Tampa FL 33620, USA^c1D Nanomaterials Group, National Institute for Material Science, 1-2-1 Sengen, Tsukuba, Ibaraki 305-0047, Japan^dSchool of Computing, Communication and Electronics, University of Plymouth, Drake Circus, Plymouth, Devon PL4 8AA, UK^eDpto. de Física de Materiales, Fac. Químicas, Universidad del País Vasco, San Sebastian 20009, Spain

ARTICLE INFO

Article history:

Available online xxx

PACS:

41.20.Jb

75.30.Gw

75.50.Kj

87.15.La

Keyword:

Devices

ABSTRACT

Structural, magnetic and mechanical properties of Co-based magnetic microwires and their composites had been investigated. It was found that annealing amorphous microwires at 600 °C caused a drastic variation in the amorphous structure due to crystallization and consequently degraded the soft magnetic properties of the microwires. The tensile tests on the single microwires of different size with and without glass-coated layer revealed a coherent correlation between the mechanical properties and the wire geometry. When compared with single magnetic microwires, the magnetic and magneto-impedance properties of composites were much improved. The strong field dependence of the effective permittivity and transmission/reflection parameters in the Gigahertz range of the composites containing short wires or arrays of continuous wires indicated that these new composites are promising candidate materials for a variety of self-sensing applications.

© 2009 Elsevier B.V. All rights reserved.

1. Introduction

Magnetic amorphous microwires have been extensively investigated in the past two decades [1–5]. The outstanding soft magnetic properties resulting from amorphous structure and small size make them suitable for a wide application in magnetic sensors [6–8], especially their giant-magneto impedance (GMI) behavior has been of much research interest for many years [1,9,10]. GMI can be understood as a small variation of external magnetic field resulting in a large change of the high frequency impedance of a ferromagnetic wire and is related to a certain magnetic structure and soft magnetic properties of the wire. The development of GMI materials falls into two trends: one is searching or designing new magnetic materials with the desired magnetic and magneto-impedance properties, and the other is aimed at improving the magnetic and magneto-impedance properties of existing materials through proper heat treatments. It has been shown that Co-based amorphous microwires are excellent candidate materials for making GMI sensors [5]. Recently, these microwires have also been used as precursors for fabricating multifunctional composite materials with electromagnetic functionalities [11].

As far as the composites are concerned, the tunable properties specifically refer to magnetic field, stress or temperature dependence of effective microwave permittivity. For the composite samples containing short magnetic wires as sensing elements or grids of parallel continuous wires, it can be irradiated by electromagnetic wave and its response can be characterized by complex effective permittivity in a resonance or relaxation dispersive manner generated by the current distribution, which may depend on the wire surface impedance [12]. Due to the existence of GMI effect, the dispersion characteristic of effective permittivity also depends on the external stimuli, such as a magnetic field or stress. These tunable properties of the composite materials afford them a wide range of applications including the field tunable microwave surfaces and the self-sensing media for the remote nondestructive test of structural materials. These composites can also be used for tunable filters and phase shifters as far as their band-structure is concerned [11–14].

In this perspective, we have designed, prepared and investigated two new types of composite consisting of Co-based magnetic microwires and fibre-reinforced 913 E-glass prepreg. One type of composite contains short magnetic microwires, while the other contains long magnetic microwires. The former demonstrates resonance type of the effective permittivity and the latter behaves as a diluted plasma. The mechanical, magnetic, magneto-impedance and microwave measurements and analyses indicate that our

* Corresponding author.

E-mail address: H.X.Peng@bristol.ac.uk (H.X. Peng).

new composites are very promising candidate materials for a variety of self-sensing applications.

2. Experimental details

2.1. Single wire

A number of Co-rich microwires with variations in composition and geometry produced by a modified Taylor–Ulitovski process were investigated. The method is capable of producing fine glass-coated metal filaments of a few μm in diameter [15,16]. The wires of composition $\text{Co}_{58.34}\text{Fe}_{3.84}\text{B}_{13.06}\text{Si}_{13.06}\text{Cr}_{11.7}$ composed of metallic core with the diameter of up to $30.8\ \mu\text{m}$ and glass coat of down to $1.5\ \mu\text{m}$ thick and suitable for MHz frequency operation were investigated after heat treatment. The heat-treatment was conducted with the samples capsulated in vacuum glass tubes in the conventional furnace at a temperature range of $300\text{--}600\ ^\circ\text{C}$ for 2 h followed by air cooling to the room temperature. Scanning electron microscopes (SEM HITACHI S-5500 & JEOL JSM-6500) were used for examining the samples prepared by cross-section polishing and mechanical polishing, respectively. X-ray diffraction (XRD) patterns were obtained using RINT 2500 with Cu $K\alpha$ radiation. SQUID was employed to undertake the magnetic test in the magnetic field parallel to the axis of the wire. Texture analyzer served the purpose of the single-wire tensile test for both glass-coated and glass-removed (by HF acid) magnetic wires with different metallic core and glass-coat thickness.

2.2. Composite preparation

For composites showing tunable properties at microwaves, thinner wires are more appropriate. We have used the wires of composition $\text{Co}_{68.7}\text{Fe}_4\text{Ni}_1\text{B}_{13}\text{Si}_{11}\text{Mo}_{2.3}$ with metallic core diameter of $17.6\ \mu\text{m}$ and glass coat thickness of $3.3\ \mu\text{m}$ as inclusions. The prepreg 913 was used as the matrix. Two types of the wire-composite systems were made. The preparation work of the short-wire composite was done in the following steps:

- (1) Five centimeter wire-pieces were laid out at zero degree along the glass-fibre direction between the two layers of prepregs with in-plane size of $50\ \text{cm} \times 50\ \text{cm}$. The wire spacing was controlled at $1.5\text{--}2\ \text{cm}$ in perpendicular direction and $3\ \text{cm}$ in the parallel direction as shown in Fig. 1.

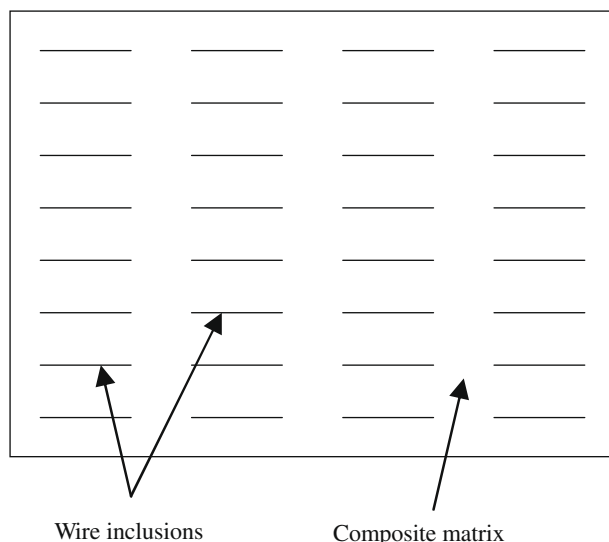


Fig. 1. Schematic graph of the short-wire composites.

- (2) Another two layers were laid up on the top and bottom of the wire-embedded layers in the same direction, giving a layout of four prepreg layers containing short wires.
- (3) After bagging the composite on an aluminum plate with air sucked out to the required vacuum of $28\text{--}31$ inchHg, the material was cured in an autoclave. The curing conditions were as follows: the temperature was raised at a rate of $2\ ^\circ\text{C}/\text{min}$ to $127\ ^\circ\text{C}$ and kept for 80 min before cooling down naturally to room temperature. At a rate of $10\ \text{psi}/\text{min}$ the pressure was increased to 30 psi and kept at this level for 30 s and then 100 psi for 600 min before decreasing at a rate of $3\ \text{psi}/\text{min}$.

The same procedure was taken for preparing long-wire composites except for that the 50 cm long wire requires spacing control only in the perpendicular direction. It is noted that the reason for using four prepreg layers is to make this composite as thin as possible, which is a necessity for the majority of targeted applications. The application of this kind of composite as microwave cover for the wave passage, for example, cannot function properly unless it is thin enough to overcome the strong energy absorption. The thickness of the final composite is around $640\ \mu\text{m}$.

3. Results and discussion

3.1. Single wire

3.1.1. Structure and magnetic properties

SEM images obtained on the samples cross-section give a clear view of the microwire which is composed of a distinct metallic core and a glass coat (Fig. 2). Also, the Taylor–Ulitovski technique employed to prepare these wires proved to be very effective in obtaining uniform evenness of the metallic core and glass-coat, as well as the good bonding between them as shown in Fig. 2.

In order to study the relationship of soft magnetic performance and structure modified by heat-treatment, the samples were annealed at temperatures ranging from 300 to $600\ ^\circ\text{C}$. Annealing at $600\ ^\circ\text{C}$ was found to be effective to induce the crystallization of the amorphous structure in our experiment. The impact on the structure caused by annealing is characterized by using both SEM and XRD. Fig. 3 shows that the surface in the cross-section of as-prepared wire becomes rough after annealing with large particles formed on it, indicating the occurrence of crystallization. This is

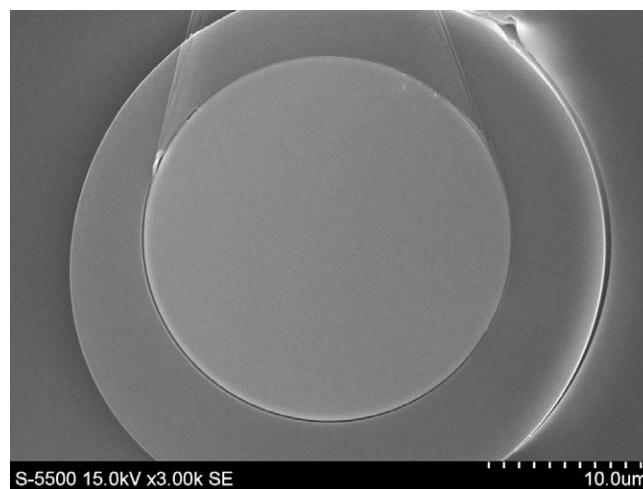


Fig. 2. Cross section view of amorphous glass-coated $\text{Co}_{58.34}\text{Fe}_{3.84}\text{B}_{13.06}\text{Si}_{13.06}\text{Cr}_{11.7}$ composed of metallic core with the diameter of $30.8\ \mu\text{m}$ and glass coat of $1.5\ \mu\text{m}$ thick.

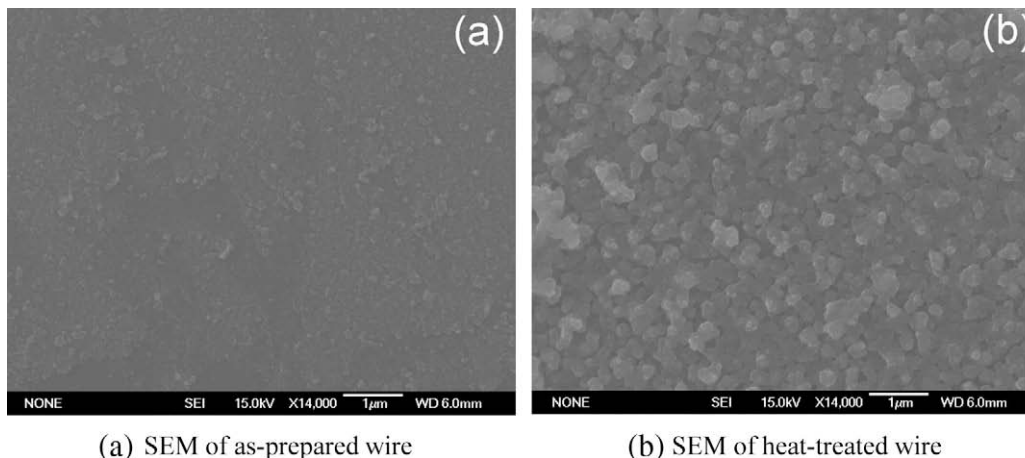


Fig. 3. Cross-section SEM images of $\text{Co}_{58.34}\text{Fe}_{3.84}\text{B}_{13.06}\text{Si}_{13.06}\text{Cr}_{11.7}$: (a) as prepared; (b) heat-treated at 600°C for 2 h.

further confirmed by the XRD tests on the glass-removed micro-wires before and after annealing as shown in Fig. 4, in which a sharp contrast of peak shape can be seen. The broad peak in the XRD pattern for as-prepared wire confirms its amorphous structure. After annealing, a stronger and narrower peak is seen at 44.5° corresponding to the Fe–Cr crystal (110) facet, indicating the formation of crystalline grains.

As a direct consequence of crystallization, the magnetic properties of the microwires annealed at 600°C were significantly modified, as shown in Fig. 5. The decrease of permeability and saturation magnetization and increase of coercivity can be understood as follows: the large particles formed, which act as pinning centers to impede the movement of domain wall, lead to the increase of coercivity and correspondingly diminish the soft magnetic properties of the wire. Another affecting factor is the formation of crystalline anisotropy resulting in significant variations in the circumferential anisotropy of the Co-based wires under the influence of high-temperature heat-treatment. As Co-based magnetic wires has a circular domain structure in the outer layer induced by the coupling of the frozen-in stress during fabrication and negative magnetostriction, annealing can also relieve the stress and hence modify the original domain structure, resulting in the change of the magnetic softness. It is noteworthy to mention that the circular domain structure of the wire is also verified here

because the linear shape of M – H curve for the as-prepared wire excludes the existence of a longitudinal anisotropy and demonstrates the existence of a preferred circumferential anisotropy accordingly.

3.1.2. Tensile properties

Four wire samples with different size were tested by the texture analyzer, and the tensile properties obtained are summarized in Table 1. After processing these data in terms of such parameters as the diameter of the metallic core (d), the thickness of the glass-coat (t) and the metal-to-glass ratio (d/t), it is found that the Young's modulus is related to the diameter of the metallic core and the rupture strength is related to the metal-to-glass ratio. In this case, the Young's modulus of a glass-coated wire E_c can be expressed via the Young's modulus of glass coat (E_g) and of metal core (E_m) as:

$$E_c = V_g E_g + V_m E_m, \quad (1)$$

where V_g , V_m are the volume percentage of the glass-coat and metal core, respectively. The volume fraction of the metallic core is about 83% of the whole wire. Therefore, the Young's modulus is supposed to be close to the value of the metallic wire. The rupture strength is heavily influenced by the metal-to-glass ratio. A larger value of metal-to-glass ratio usually corresponds to a higher tensile strength [17].

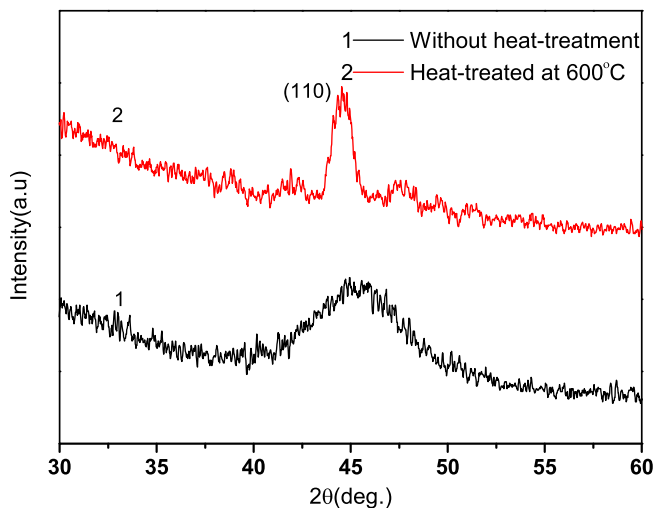


Fig. 4. X-ray diffraction patterns of the glass-removed $\text{Co}_{58.34}\text{Fe}_{3.84}\text{B}_{13.06}\text{Si}_{13.06}\text{Cr}_{11.7}$ wire before and after heat-treated at 600°C .

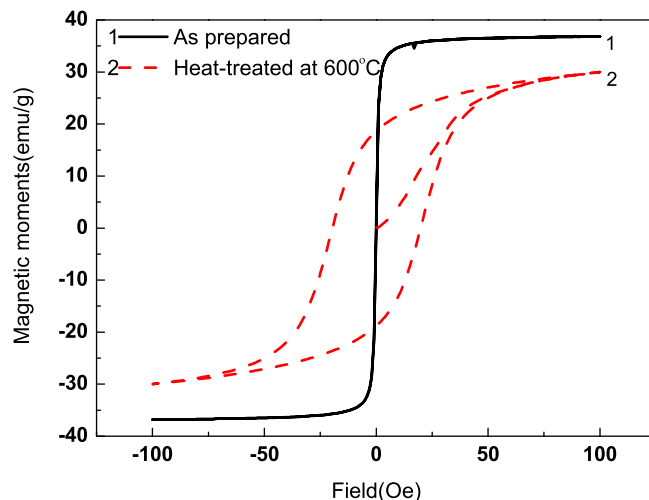


Fig. 5. M – H curves of the as-prepared $\text{Co}_{58.34}\text{Fe}_{3.84}\text{B}_{13.06}\text{Si}_{13.06}\text{Cr}_{11.7}$ wire and the heat-treated at 600°C measured in horizontal field.

Table 1
Geometrical parameters and mechanical properties of glass-coated $\text{Co}_{58.34}\text{Fe}_{3.84}\text{B}_{13.06}\text{Si}_{13.06}\text{Cr}_{11.7}$ wires.

Sample No. (#)	Diameter of metallic core ($d/\mu\text{m}$)	Glass coat thickness ($t/\mu\text{m}$)	d/t	Young's modulus (GPa)	Rupture strength (MPa)
1	9.9	1.88	5.27	77.4	920
2	15.2	4.2	3.62	98.1	563
3	17.4	1	17.4	125.6	1779
4	17.6	3.3	5.33	142.9	928

Table 2
Mechanical properties of glass-removed $\text{Co}_{58.34}\text{Fe}_{3.84}\text{B}_{13.06}\text{Si}_{13.06}\text{Cr}_{11.7}$ wires with different diameter.

Sample Number(#)	Young's modulus (GPa)	Rupture strength (MPa)
1	46.2	1057
2	65.4	1259
3	92.5	1737
4	163.4	3601

Tensile tests were also conducted on the glass-removed wires in order to make a comparative study with the glass-coated wires. These data also provided usefulness for the preparation of the corresponding composites. The glass coats were removed using HF acid (47%). The tensile test results are summarized in Table 2.

Comparing Table 1 with Table 2, the overall influence of the glass-removal is that the glass-removal decreases the Young's modulus but increases the rupture strength. A better flexibility of the metal is attained when it is freed from the glass-coat, thus improving its performance to the external stress, which is reflected in the decrease of the Young's modulus. The Young's modulus dependency on the diameter of the wires remain the same as that for the glass-coated wire.

Large values of GMI effect in Co-based wires owe to a well established circumferential anisotropy and its relatively low values with the effective anisotropy field H_K in the range of a few Oe. This stress-induced anisotropy can be also controlled by metal-to-glass ratio. This is a simple one-step process allowing a strict control of properties in as-cast state and optimization of the MI characteristics. Fig. 6 [18] shows the MI ratio versus external field for different values of $\rho = d/D_w$ where D_w is the total wire diameter. For a very thin glass layer, the MI ratio reaches 600% for a field of about 1 Oe at a frequency of 10 MHz. This is the best result reported so far for any GMI system. The GMI in these wires can be made very sensitive to stresses as well. Very large values of MI ratio can be obtained even at GHz frequencies as shown in Fig. 7 [19] which justifies the use of GMI wires as inclusions in composites to achieve electromagnetic functionalities at microwave frequencies.

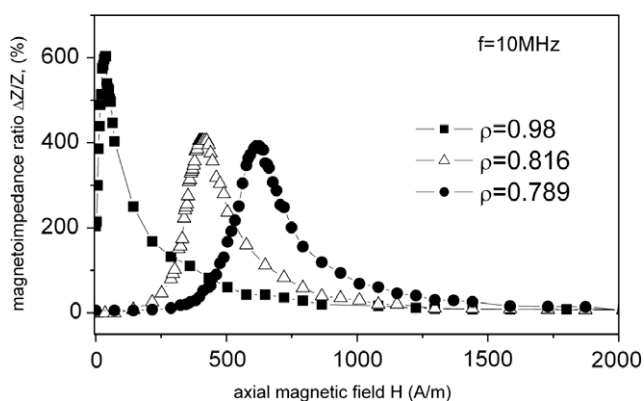


Fig. 6. MI ratio plots in $\text{Co}_{67}\text{Fe}_{3.85}\text{Ni}_{1.45}\text{B}_{11.5}\text{Si}_{14.5}\text{Mo}_{1.7}$ glass-coated wires for different values of ρ . The wire diameter is about $22\ \mu\text{m}$.

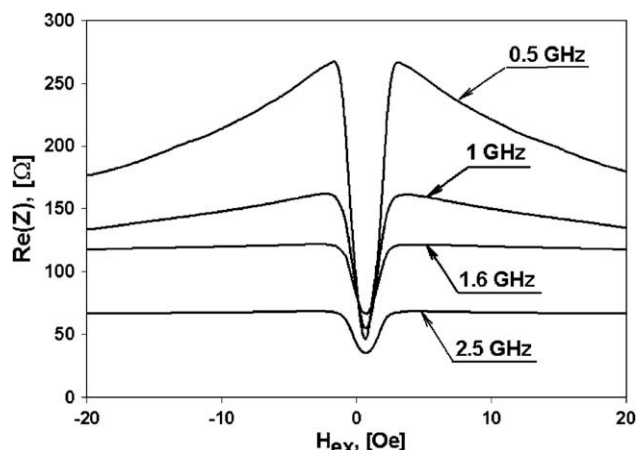


Fig. 7. Field dependence of real part of impedance in glass-coated Co-rich wires at 0.5–2.2 GHz.

3.2. Multifunctional macro-composites

3.2.1. DC magnetic properties and GMI effect

Composites used to investigate GMI effect were prepared by embedding the wires in the composite matrix in a parallel manner. The interaction between the wires does not result in the increase of the anisotropy and even slightly reduces the coercivity, resulting in better soft magnetic properties as shown in Fig. 8 [20]. The impedance of the whole composite sample can be investigated. In this case, the increase of the number and decrease of the length of wires resulted in a large enhancement of GMI effect and field sensitivity and this is mainly due to increase of overall conductivity of the samples. Fig. 9 shows that, at a given frequency of 10 MHz, the GMI ratio and its field sensitivity reached the highest values of 450% and 45%/Oe for those composites containing four wires, while the one containing only one wire gave 14% and 1%/Oe, respectively. According to our previous work, the GMI ratio increased from 15.5% to 268% as the microwire length decreased from 4 to 1 mm [21]. These results are of vital significance to the sensor application in terms of its preferred small size and high sensitivity.

3.2.2. Microwave tunable properties

The study of tunable microwave response from wire-composites was conducted by modeling the effective permittivity and free-space measurement of the transmission/reflection spectra in the presence of external magnetic field.

The composites containing short pieces of microwires are characterized by resonance type of the effective permittivity as the wires behave as dipole antennas with the resonance at half wave length condition:

$$f_{\text{res}} = \frac{c}{2L\epsilon} \quad (2)$$

where L is the wire length, c is the velocity of light and ϵ is the permittivity of matrix. For our composites, ϵ is about 2, so the wire length of 5 cm corresponds to a resonance frequency of about 2 GHz where the GMI effect is large. The results of modeling of

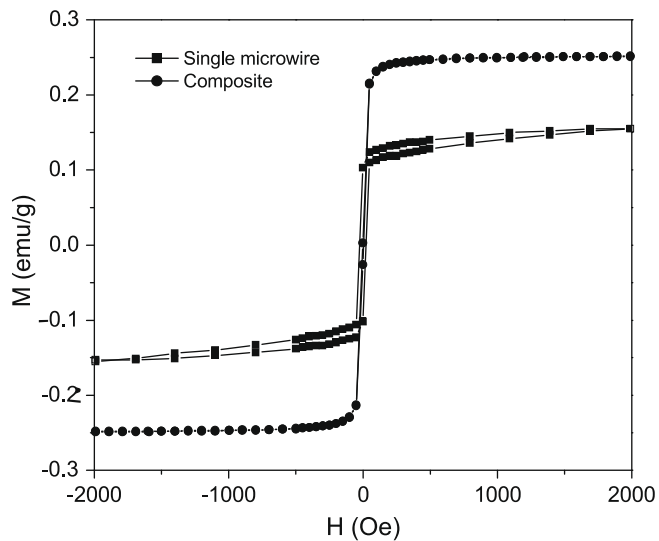


Fig. 8. Comparison of magnetic hysteresis loops of single magnetic microwire and as-prepared composite.

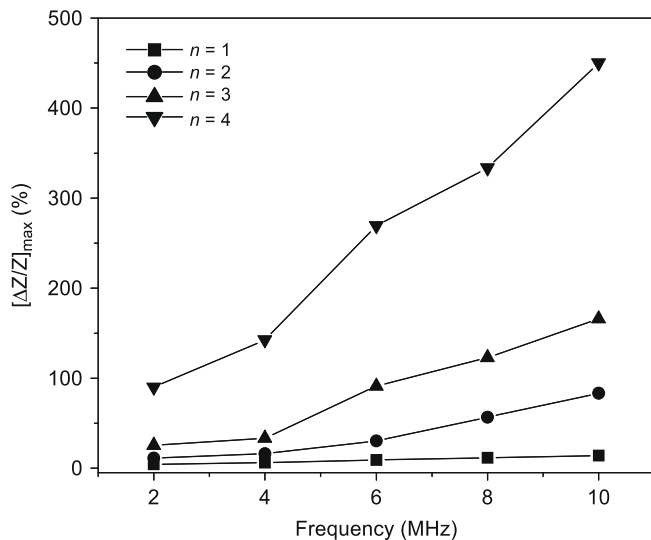


Fig. 9. The frequency dependency of the maximum GMI ratio, $[\Delta Z/Z]_{max}$, for samples with different numbers of wire (n).

the effective permittivity for the present system is shown in Fig. 10 (the method is explained in Refs. [11,12]). It is seen that in the presence of external field the resonance becomes very broad since losses are increased in high impedance state of the wires.

In the case of composites with continuous wires, the dispersion of the effective permittivity corresponds to that for a diluted plasma [22] with a characteristic plasma frequency:

$$f_p^2 = \frac{c^2}{2\pi b^2 \ln(b/a)} \quad (3)$$

where b is the spacing between the wires and a is the wire radius. We have modeled this permittivity for the case of magnetic wires taking into account the wire impedance as shown in Fig. 11. Choosing the values of $b = 1.5$ cm and $a = 10$ μm , the plasma frequency is about 3 GHz. Below this frequency, the real part of the permittivity is negative with the absolute value strongly decreasing with increasing field due to improvement in the impedance of the wires. Therefore, we can conclude that for both types of composites there

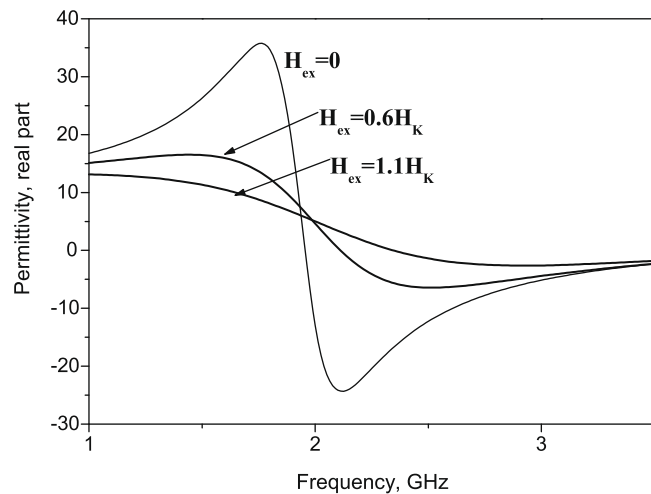


Fig. 10. Frequency plots of the effective permittivity, real part, for composites containing short wires with the external field H_{ex} as a parameter. Other parameters used for modeling are: $H_K = 7$ Oe, saturation magnetization $M_s = 500$ G, wire radius $a = 10$ μm , wire length $L = 5$ cm, wire electrical conductivity 10^{16} s^{-1} , volume concentration of wires $p = 0.02\%$, the permittivity of matrix $\epsilon = 2.2$.

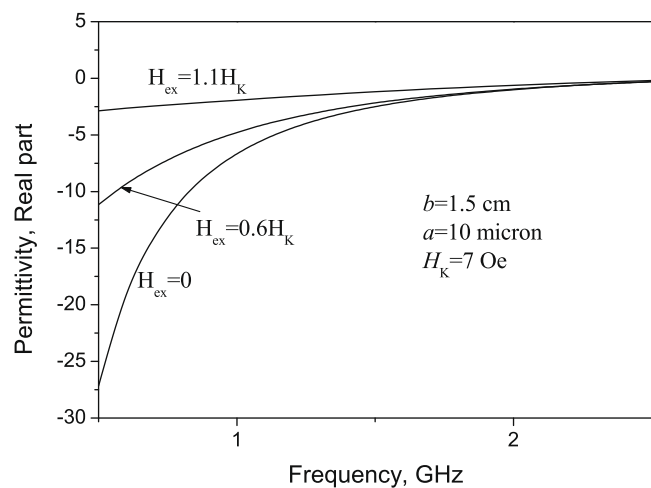


Fig. 11. Frequency plots of the effective permittivity, real part, for composites containing continuous wires with the external field H_{ex} as a parameter. Geometrical parameters are: spacing between wires $b = 1.5$ cm, wire radius $a = 10$ μm . The magnetic and electrical parameters are the same with those for Fig. 10.

is a strong dependence of the effective permittivity on the external field the application of which increases the microwave impedance of wires, and hence, the losses in the system. As a result, the microwave response in such composites depends on the external field.

The modeling results on transmission/reflection parameters for resonance type composite are shown in Fig. 12(a) and (b) for the parameters corresponding to the experimental samples ($L = 5$ cm, D – sample thickness = 650 μm , $H_K = 7$ Oe, M_s – magnetization saturation = 500 G). Fig. 12(a) shows the transmission spectra with a deep minimum at the resonance frequency, which is strongly reduced by the application of external field. In the case of a reflection parameter, the interest may be related with the phase which approaches $\pm 180^\circ$ in the vicinity of resonance as shown in Fig. 12(b). Note that unlike reconfigurable frequency selective surfaces (see, for example, [23]), in our case the phase does not go through 0° as $\pm 180^\circ$ is the same point of a periodic phase function without a discontinuity but this point can be detected and it experiences a frequency shift in the presence of the field.

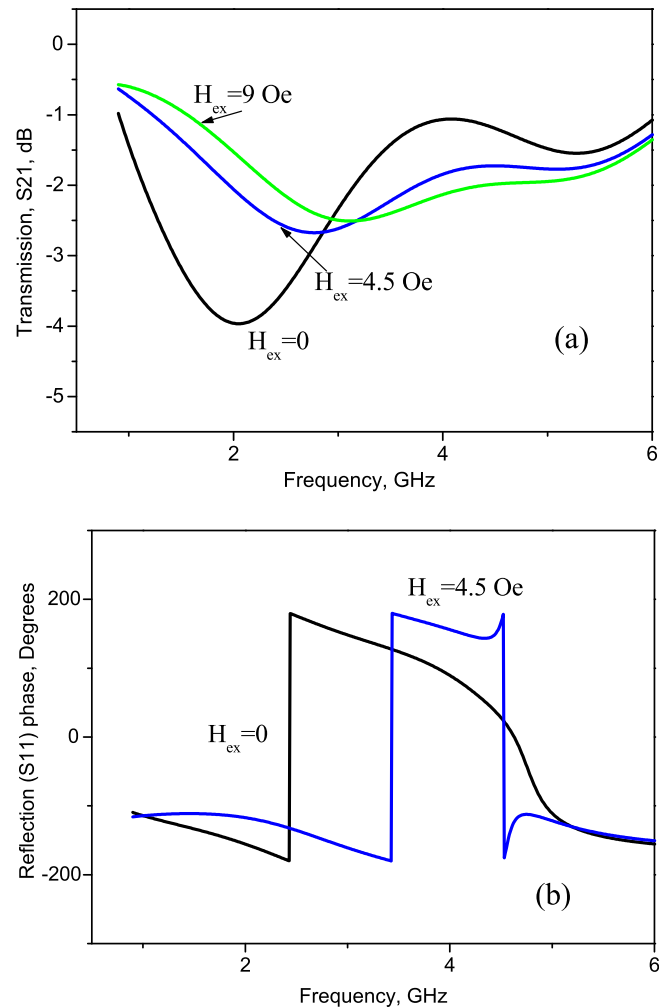
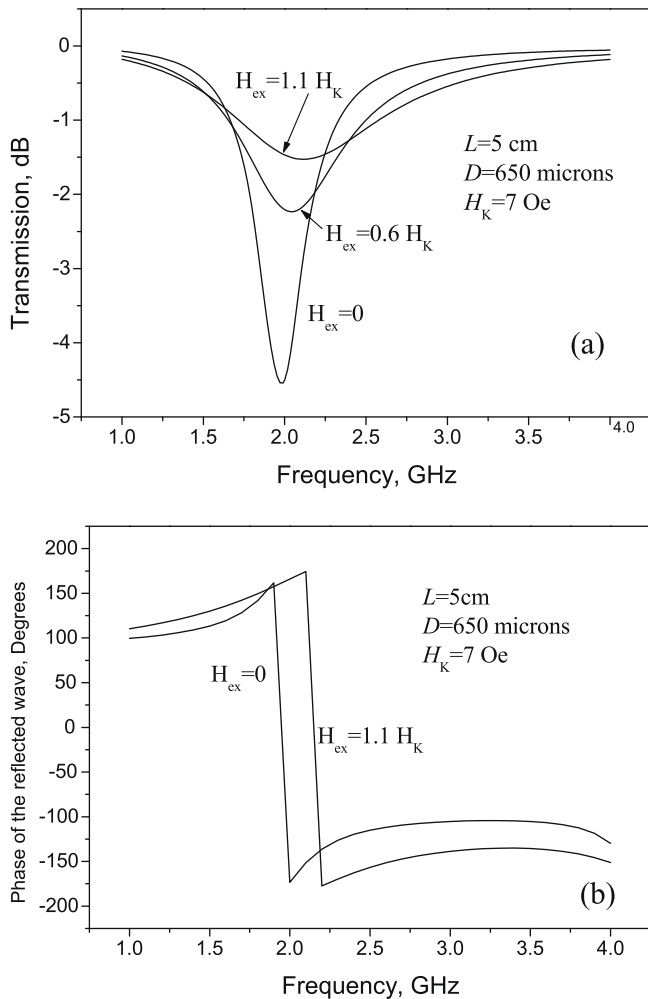


Fig. 12. Theoretical transmission/reflection spectra for composite slab with thickness of 650 μm containing short pieces of magnetic wires using results of the permittivity shown in Fig. 10. (a) The amplitude of transmission parameter, and (b) the phase of the reflection parameter.

Fig. 13. Experimental transmission/reflection spectra for composite sample of 640 μm thick and 50 cm \times 50 cm in-plane size with 5 cm long amorphous wires. (a) Amplitude of transmission S21, and (b) phase of reflection S11.

The microwave responses from composite samples placed in a planar coil creating a magnetic field were measured in free space. In general, the installation includes a pair of broadband horn antennas connected to the analyzer's ports and a mini anechoic chamber covered inside with a microwave absorber. The parasitic scattering in the measuring track is reduced by employing a time-domain option, which enables the separation of the useful signal from background. The details can be found elsewhere [14].

Fig. 13(a) and (b) show the transmission amplitude (amplitude of S21-parameter) and phase of the reflection parameter (phase of S11-parameter) for composites with 5 cm wire long pieces in the presence of external magnetic field. In accordance with the results of theoretical modeling, the transmission parameter has a minimum near a frequency of 2 GHz which broadens with increasing the field and the minimum shifts to higher frequencies. At resonance, transmission increases from -4 dB when there is no external field H_{ex} to -2.5 dB for $H_{\text{ex}} = 9$ Oe. For such thin composite samples (640 μm), larger impact of the field on microwave response would require a material with higher concentration of the wires. In the present case, the wire volume concentration is about 0.02%. The frequency at which the phase goes through $\pm\pi$ also shifts to the right in the presence of the field from 2.4 GHz for $H_{\text{ex}} = 0$ to 3.5 GHz for $H_{\text{ex}} = 4.5$ Oe. This is a significant change which is convenient to use for sensing applications such as

stress/temperature monitoring. The experimental results quantitatively agree with the theory at lower frequencies and there is a discrepancy at higher frequencies. This could be associated with a larger influence of scattering in the measurement track at higher frequencies when a frequency dependent time domain gating is required. However, there is no noticeable field dependency of the reflection/transmission parameters at frequencies higher than 5 GHz (outside of the dispersion area for the effective permittivity).

In the case of composites containing long continuous wires, its microwave spectrum (Fig. 14) has different features compared to that of the composites containing short wires due to the fact that the absence of charge distribution in the long wires and associated resonances perforce result in a different electromagnetic response with the effective permittivity of plasma type (see Fig. 11). Nevertheless, the strong field dependence of transmission/reflection parameters also exists for frequencies below and near the plasma frequency. In this case, the application of external field may decrease the transmission parameter due to the rise of absorption as shown in Fig. 14(a). At a frequency around a plasma frequency of 3 GHz the transmission decreases from -1.5 dB at $H_{\text{ex}} = 0$ to -3.2 dB for $H_{\text{ex}} = 9$ Oe. The reflection amplitude shown in Fig. 14(b) demonstrates significant decrease with the field at lower frequency band from -4 dB for $H_{\text{ex}} = 0$ to -12 dB for $H_{\text{ex}} = 9$ Oe, since the effective permittivity decreases in absolute terms. Such behavior would be of interest for sensing applications as well. With

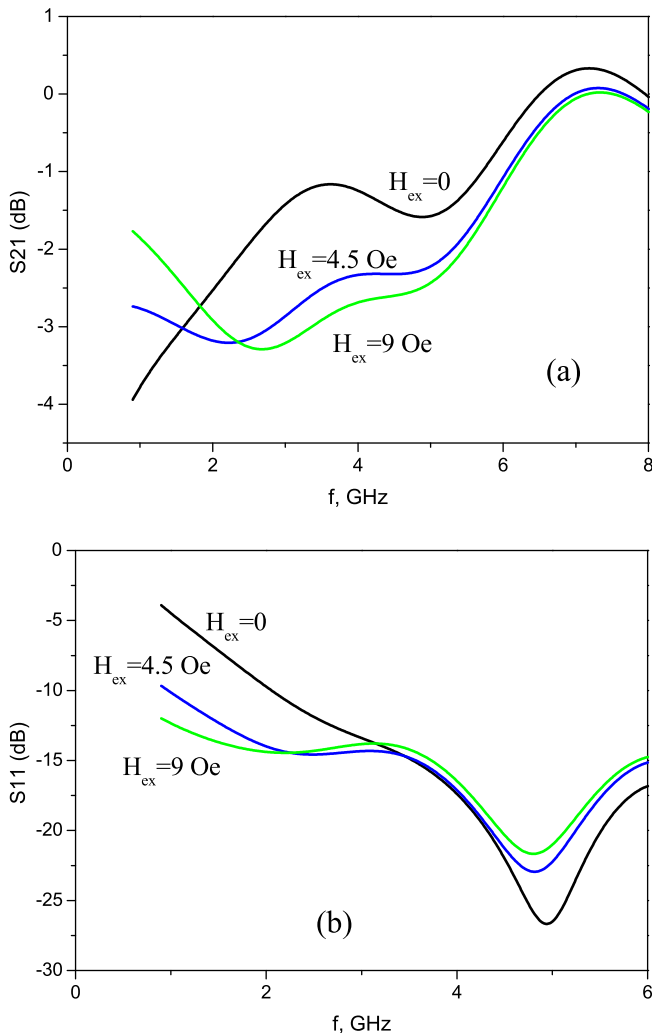


Fig. 14. Experimental transmission/reflection spectra for composite sample of 640 μm thick and 50 cm \times 50 cm in-plane size with continuous amorphous wires spaced at 1.5–2 cm. (a) Amplitude of transmission S_{21} , and (b) amplitude of reflection S_{11} .

increasing frequency, there exists additional band showing the field effect the origin of which is not clear.

4. Conclusions

We have systematically investigated the structural, magnetic, magneto-impedance, mechanical and microwave properties of Co-based magnetic microwires and the composites containing these microwires. The magnetic properties of the microwires are associated with their magnetic domain structure that can be modified by annealing treatment. There is a coherent correlation between the mechanical properties and the wire geometry. A great enhancement in the GMI effect has been achieved by changing the wire geometry in the composites containing long wires, indi-

cating that these wires and composites are very promising for GMI sensor applications. The strong field dependence of the effective permittivity of the composites containing short wires and long continuous wires indicates that these composites are potential candidate materials for a wide range of self-sensing applications.

Acknowledgement

HXP would like to acknowledge the financial support from the Engineering and Physical Science Research Council (EPSRC) UK under the Grant No. EP/FO3850X. Mr F. Qin is supported through Overseas Research Students Awards Scheme (ORSAS) and University of Bristol Postgraduate Student Scholarship. Part of experimental work on characterizations was carried out in the National Institute for Material Science (NIMS) where Mr Qin was awarded an internship certificate and “Nanotechnology Network Project” of the Ministry of Education, Culture, Sports, Science and Technology (MEXT), Japan. The authors also acknowledge valuable discussions with Dr Makhnovskiy of Plymouth University and his help in designing the free space measurement installation.

References

- [1] L.V. Panina, K. Mohri, Appl. Phys. Lett. 65 (9) (1994) 1189.
- [2] P.T. Squire, D. Atkinson, M.R.J. Gibbs, S. Atalay, J. Magn. Magn. Mater. 132 (1–3) (1994) 10.
- [3] H. Chiriac, T.A. Ovari, Prog. Mater. Sci. 40 (5) (1996) 333.
- [4] A. Zhukov, V. Zhukova, J.M. Blanco, A.F. Cobeno, M. Vazquez, J. Gonzalez, J. Magn. Magn. Mater. 258&259 (2003) 151.
- [5] M.H. Phan, H.X. Peng, Prog. Mater. Sci. 53 (2) (2008) 323.
- [6] H. Chiriac, C.S. Marinescu, T.A. Ovari, Maria Neagu, Sens. Actuators A: Phys. 76 (1–3) (1999) 208.
- [7] D. Atkinson, P.T. Squire, M.G. Maylin, J. Gore, Sens. Actuators A: Phys. 81 (1–3) (2000) 82.
- [8] M. Tibu, H. Chiriac, J. Magn. Magn. Mater. 320 (20) (2008) e939.
- [9] L.V. Panina, K. Mohri, T. Uchiyama, K. Noda, M. Bushida, IEEE Trans. Magn. 31 (2) (1995) 1249.
- [10] V. Zhukova, M. Ipatov, A. Zhukov, J. Gonzalez, J.M. Blanco, Sens. Actuators B: Chem. 126 (1) (2007) 232.
- [11] D.P. Makhnovskiy, L.V. Panina, Field and stress tunable microwave composite materials based on ferromagnetic wires, in: V.N. Murray (Ed.), Progress in Ferromagnetism Research, Nova Science Publishers Inc., Hauppauge, NY, 2005.
- [12] D.P. Makhnovskiy, L.V. Panina, J. Appl. Phys. 93 (7) (2003) 4120.
- [13] L.V. Panina, Dmitriy P. Makhnovskiy, Kaneo Mohri, J. Magn. Magn. Mater. 272–276 (Part 2) (2004) 1452.
- [14] D.P. Makhnovskiy, L.V. Panina, C. Garcia, A.P. Zhukov, J. Gonzalez, Phys. Rev. B (Condens. Matter Mater. Phys.) 74 (6) (2006) 064205.
- [15] G.F. Taylor, Phys. Rev. 23 (5) (1924) 655.
- [16] N.M. Avernin, A.V. Ulitovski, Method of fabrication of metallic microwire. Patent No. 161325 (USSR), 19.03.64, Bulletin No. 7, p. 14.
- [17] H. Montiel, G. Alvarez, M.P. Gutierrez, R. Zamorano, R. Valenzuela, IEEE Trans. Magn. 42 (10) (2006) 3380.
- [18] V. Zhukova, A. Chizhik, A. Zhukov, A. Torcunov, V. Larin, J. Gonzalez, IEEE Trans. Magn. 38 (5) (2002) 3090.
- [19] S.I. Sandacci, D.P. Makhnovskiy, L.V. Panina, J. Magn. Magn. Mater. 272–276 (Part 3) (2004) 1855.
- [20] M.H. Phan, H.X. Peng, S.C. Yu, M.R. Wisnom, J. Magn. Magn. Mater. 316 (2) (2007) e253.
- [21] M.H. Phan, H.X. Peng, M.R. Wisnom, P.H. Mellor, Optimizing the nanostructure of magnetic micro-wires for multifunctional macro-composites, AIAA-2007-2032, in: 48th AIAA/ASME/ASCE/AHS/ASC Structures, Structural Dynamics, and Materials Conference, Honolulu, Hawaii, April 23–26, 2007.
- [22] J.B. Pendry, A.J. Holden, W.J. Stewart, I. Youngs, Phys. Rev. Lett. 76 (25) (1996) 4773.
- [23] D. Sievenpiper, J. Schaffner, R. Loo, G. Tagonan, S. Ontiveros, R. Harold, IEEE Trans. Antennas Propagation 50 (3) (2002) 384.